COMMUNICATION

Nanoscale stabilization of the scheelite-type structure in La$_{0.99}$Ca$_{0.01}$NbO$_4$ thin films

Cristina Tealdi,* Eliana Quartarone, Piercarlo Mustarelli and Lorenzo Malavasi*

In this paper we report on the deposition of La$_{0.99}$Ca$_{0.01}$NbO$_4$ thin films with scheelite-type crystal structure. Thanks to the film's nanostructure, we were able to stabilize the tetragonal scheelite-type structure phase at room temperature, which involves a full removal of the fergusonite–scheelite phase transition.

There is a strong interest in the study of proton conducting oxides that could overcome the drawbacks of Y-doped BaCeO$_3$ which, at present, is the state-of-the-art electrolyte for intermediate temperature fuel cells (IT-SOFC).[1] Doped *ortho*-niobates and tantalates of general formula RE(Ta,Nb)O$_4$ (RE = rare earth) have proton conductivity in the order of 10^{-3} Ω^{-1} cm^{-1} above 700 °C with good stability under CO$_2$-rich atmosphere,[2] where perovskite-type Sr and Ba cerates typically suffer from material decomposition, even at low CO$_2$ levels.[3] In addition, the pure proton conductivity of doped *ortho*-niobates and tantalates makes these materials interesting for hydrogen and humidity sensors at temperatures below 700 °C.[2] Among the *ortho*-niobates investigated in the current literature, the highest ionic conductivity coupled to the highest proton mobility has been observed for 1% Ca-doped LaNbO$_4$.[2,4]
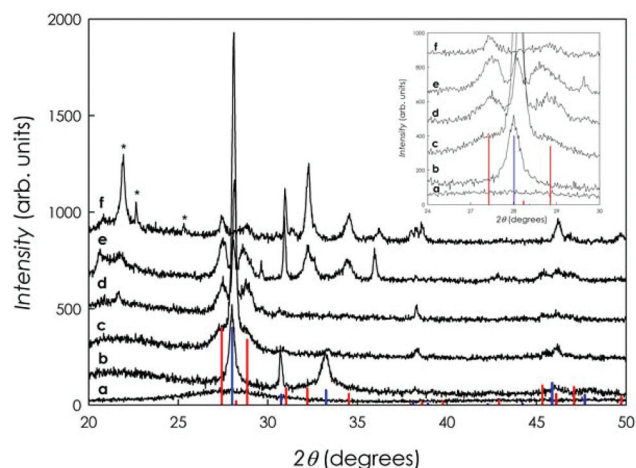
From the structural point of view, La$_{0.99}$Ca$_{0.01}$NbO$_4$ possesses a low temperature monoclinic phase with the fergusonite-type structure and a high temperature scheelite-like structure above *ca.* 495 °C.[5] This phase transition is accompanied by a large change in thermal expansion.[5,6] It is clear that the presence of a phase transition in the operation temperature range of La$_{0.99}$Ca$_{0.01}$NbO$_4$ is concerning. The strategies proposed to address the phase transition problem may involve the stabilization, at high temperature, of the low-*T* fergusonite polymorph. However, this will in turn reduce the proton conductivity since the activation energy for proton mobility in the fergusonite structure is 0.73–0.83 eV while in the scheelite structure it is 0.52–0.62 eV.[2,4] Clearly, it would be highly desirable to remove the phase transition in the operation temperature range of La$_{0.99}$Ca$_{0.01}$NbO$_4$ while preserving

the highly conducting scheelite structure in the whole *T*-range. This result requires the stabilization of the tetragonal scheelite-type polymorph at low temperatures. It was proposed that the retention of the high-temperature polymorph at lower temperatures is most likely induced by reduction of the B-site cation.[7] Brandao *et al.* recently verified this result on highly V-doped La$_{0.98}$Sr$_{0.02}$NbO$_4$.[8,9] In addition, V-doped lanthanum niobates were the subject of earlier studies suggesting that surface control and finite particle size effects can lower the fergusonite–scheelite transformation temperature also by over a hundred degrees, inducing the coexistence of the high and low temperature phases in a range of temperatures.[10,11] However, further experimental results on the stabilization of the scheelite polymorph are not yet present in the current literature and, in particular, there are no reports related to La$_{0.99}$Ca$_{0.01}$NbO$_4$.

In this Communication we have shown the possibility of stabilizing the tetragonal scheelite polymorph at low temperature in La$_{0.99}$Ca$_{0.01}$NbO$_4$. This result was obtained on thin films because La$_{0.99}$Ca$_{0.01}$NbO$_4$ has a relatively low conductivity (although purely protonic) which requires the electrolyte thickness to be ~1 μm to meet area-specific resistances around 0.1 Ω cm^2. Among the current literature on La$_{0.99}$Ca$_{0.01}$NbO$_4$ thin films preparation, only Magraso *et al.*[12] and Cavallaro *et al.*[13] reported films with the required thickness for exploitable IT-SOFC performances. However, the crystal structure of these films is of the monoclinic fergusonite-type. The thin films of La$_{0.99}$Ca$_{0.01}$NbO$_4$ investigated in the present work were deposited on amorphous silica substrates by means of radio frequency (RF) magnetron sputtering, starting from La$_{0.99}$Ca$_{0.01}$NbO$_4$ powders synthesized by solid-state reaction, as described elsewhere.[5] Starting powders showed the usual monoclinic crystal structure at room temperature (RT).[5] For all the films deposition the RF power was set to 150 W, deposition time was 5 h and argon pressure in the chamber was 2×10^{-2} mbar. The substrate was not heated during thin films preparation. Different post-deposition thermal treatments were carried out on the deposited films. In particular, we applied a heating ramp (5 °C min^{-1}) from RT to 700, 800, 900, 1000 and 1200 °C; after reaching the set temperature the samples were

Department of Chemistry and INSTM, Viale Taramelli 16, I-27100 Pavia, Italy.
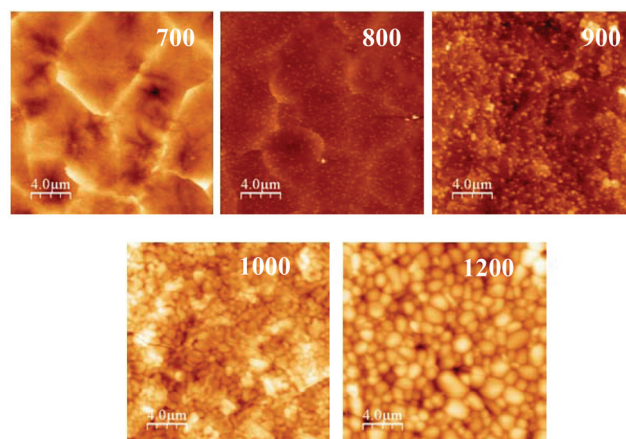*E-mail: cristina.tealdi@unipv.it, lorenzo.malavasi@unipv.it*

Fig. 1 XRD patterns for the $La_{0.99}Ca_{0.01}NbO_4$ thin films deposited. Pattern (a) refers to a film deposited at 700 °C without annealing. Patterns (b)–(f) refer to thin films annealed at 700, 800, 900, 1000 and 1200 °C, respectively. Inset: detailed view of XRD patterns around the main peaks.

Fig. 2 AFM images (20 μm × 20 μm) for the $La_{0.99}Ca_{0.01}NbO_4$ thin films annealed at 700, 800, 900, 1000 and 1200 °C, respectively.

Fig. 3 AFM images (700, 800: 2 μm × 2 μm; 900: 5 μm × 5 μm) for the $La_{0.99}Ca_{0.01}NbO_4$ thin films annealed at 700, 800, 900 °C, respectively.

kept under isothermal conditions for 2 h and then slowly cooled (1 °C min⁻¹) down to RT. Thin films thickness, as determined using a mechanical profilometer, was around 0.5 μm. X-ray diffraction (XRD) patterns were acquired with a D8 Advance (Bruker) diffractometer (Cu-radiation). The AFM images were collected with an Autoprobe CP Research Microscope (Thermomicroscope-VEECO), operating in the contact mode, by means of sharpened pyramidal silicon tip (curvature radius <20 nm) onto rectangular microlevers (force constant, 0.03 N m⁻¹) (Thermomicroscope-VEECO). For each analysed sample, scans of different areas were carried out at a scan rate of 0.7–1.0 Hz. The nanoparticle dimensions were calculated by analysing at least 20 line profiles.
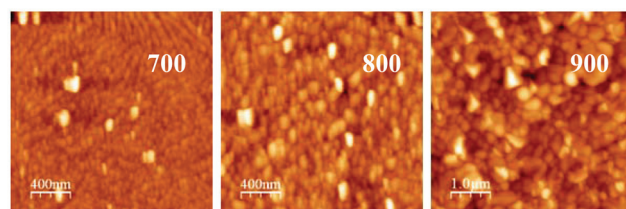
Fig. 1 reports the XRD patterns of the $La_{0.99}Ca_{0.01}NbO_4$ thin films deposited as described above, while red and blue vertical bars refer to the theoretical Bragg peaks for the fergusonite and scheelite crystal structures, respectively.

Pattern (a) refers to a film grown while heating the substrate at 700 °C and without any post-deposition annealing. As can be seen from Fig. 1, this film is completely amorphous. Patterns (b)–(f) refer to films deposited without substrate heating, which underwent post-deposition thermal treatments at 700, 800, 900, 1000 and 1200 °C, respectively. In these cases, the films were well crystallized and display XRD patterns fully compatible with the lanthanum niobate polymorphs.

From the analysis of the collected XRD patterns, it can be observed that the $La_{0.99}Ca_{0.01}NbO_4$ thin film which was heated at 700 °C presents a single-phase composition in agreement with the scheelite structure. By increasing the post-deposition annealing temperature, the fergusonite phase starts to appear in the diffraction patterns, as can be seen from pattern (c). From 800 to 1200 °C the relative amount of the fergusonite phase increases and, at 1200 °C, the sample is made of single-phase fergusonite $La_{0.99}Ca_{0.01}NbO_4$. A closer view of the region

around the main peaks of the niobate polymorphs is reported in the inset of Fig. 1. Peaks marked with an asterisk in Fig. 1 refer to crystalline SiO_2 (mainly tridymite polymorph) which starts to crystallize from 900 °C. From the diffraction patterns, the very good agreement between the calculated Bragg peaks for the $La_{0.99}Ca_{0.01}NbO_4$ structures and the experimental patterns can be also observed. This is also an indication of the good stoichiometry of the samples, which was also checked by micro-probe analysis (data not shown).

Fig. 2 reports the AFM images for the (b)–(f) films in Fig. 1 for a 20 μm × 20 μm scan. Temperature inside each figure indicates the post-deposition annealing temperature.

As expected, it is possible to observe a progressive increase of the $La_{0.99}Ca_{0.01}NbO_4$ thin film's average grain size by increasing the post-deposition annealing temperature. While for the films treated at 1000 and 1200 °C the morphology is clear at this AFM scan size, for the samples treated at 700–900 °C it is difficult to define a clear morphology.

Fig. 3 shows another AFM scan for the 700–900 °C samples collected at a higher resolution and smaller scan sizes.

At this resolution it can be appreciated that the grain size for the samples treated between 700 and 900 °C is in the nanometer range with the smaller average grain size of about 25 nm for the sample annealed at 700 °C. On the other hand, as it is clear from Fig. 2, post-deposition thermal treatments at 1000 and 1200 °C led to an average grain size in the μm range.
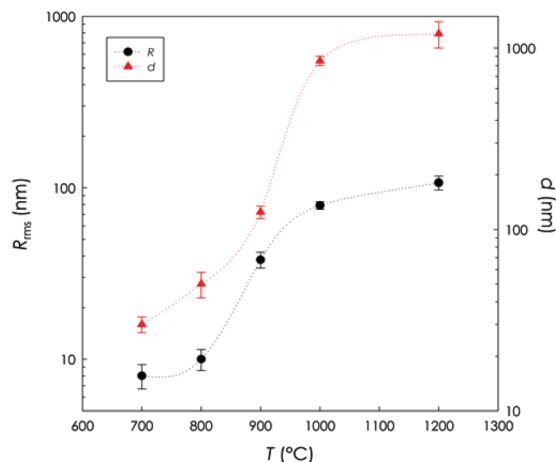
Fig. 4 Average grain size (*d*) and roughness (*R*) for the $La_{0.99}Ca_{0.01}NbO_4$ thin films annealed at 700, 800, 900, 1000 and 1200 °C, respectively.

Overall, from the AFM investigation, it appears that the morphology is more rod-like at lower temperatures and becomes more spherical on increasing the annealing temperature.

The average grain sizes and surface roughness determined from the AFM investigation are summarized in Fig. 4.

By increasing the post-deposition annealing temperature the grain size increases from about 25 nm (700 °C) to about 1 µm (1000 °C) and the average roughness increases from about 8 nm (700 °C) to more than 100 nm (1000 °C).

Conclusions

We were able to stabilize at room temperature the tetragonal scheelite structure of $La_{0.99}Ca_{0.01}NbO_4$. The origin of the stabilization of the tetragonal polymorph cannot be explained on the basis of a possible metastable stabilization of the scheelite-type structure induced by the thermal treatment, since each sample was cooled down through the phase transition with a very slow ramp (1 °C min⁻¹) which ensures the stabilization of the equilibrium phase.[5,14,15]

The most plausible explanation of the observed results can be found in the nanoscale morphology of the deposited films. It is well known that the nanostructure can alter the phase equilibria in polymorphic solid materials.[16–19] The nanostructure usually produces an inversion in the polymorphs stability, as observed in several oxides (for an extended review see ref. 19). For example, in nanocrystalline titania, the anatase structure is observed instead of rutile, while in the undoped nanocrystalline zirconia the tetragonal phase is observed, instead of the regular monoclinic phase.[19] It is now generally recognized that this inversion does not represent a pure kinetic effect, but the polymorphs present in the nanomaterials are the most stable phase for that composition.[20,21] For a given compound, therefore, a critical grain size exists below which such an inversion in the polymorphs stability takes place. In the case of zirconia, for example, this value is around 10 nm.[19] For most of

the oxides investigated in this respect, the range of inversion in the polymorphs stability is between 3 and 45 nm.[19]

According to the AFM data presented in this work, the film treated at 700 °C is made of nanoparticles having average grain size of around 25 nm, which is likely below the grain size required for the stabilization of the single tetragonal phase. When the average diameter is above *ca.* 40 nm (as in the film annealed at 800 °C) the monoclinic phase starts to show in the XRD patterns. Our results are corroborated by the evidence of a major portion of the tetragonal phase at low temperature in Ca-doped $LaNbO_4$ nanoparticles of average crystallite size of around 45 nm prepared by the freeze-dried precursor method.[22]

Acknowledgements

Notes and references

1 L. Malavasi, C. A. J. Fisher and S. M. Islam, *Chem. Soc. Rev.*, 2010, **39**, 4370.
2 R. Haugsrud and T. Norby, *Nat. Mater.*, 2006, **5**, 193.
3 K. D. Kreuer, *Annu. Rev. Mater. Res.*, 2003, **33**, 333.
4 R. Haugsrud and T. Norby, *Solid State Ionics*, 2006, **177**, 1129.
5 L. Malavasi, C. Ritter and G. Chiodelli, *J. Alloys Compd.*, 2009, **475**, L42.
6 L. Jian and C. M. Waymann, *J. Am. Ceram. Soc.*, 1997, **80**, 803.
7 J. P. Bastide, *J. Solid State Chem.*, 1987, **71**, 115.
8 A. D. Brandao, I. Atunes, J. R. Frade, J. Torre, V. V. Kharton and D. P. Fagg, *Chem. Mater.*, 2010, **22**, 6673.
9 A. D. Brandao, I. Atunes, J. R. Frade, J. Torre, S. M. Mikhalev and D. P. Fagg, *Int. J. Hydrogen Energy*, 2012, **37**(8), 7252.
10 S. K. Chan, *J. Mater. Sci. Lett.*, 1985, **4**, 862.
11 A. T. Aldred, M. V. Nevitt and S. K. Chan, *J. Mater. Sci. Lett.*, 1985, **4**, 867.
12 A. Magraso, H. Xuriguera, M. Varela, M. F. Sunding, R. Strandbakke, R. Haugsrud and T. Norby, *J. Am. Ceram. Soc.*, 2010, **93**, 1874.
13 A. Cavallaro, C. Solis, P. R. Garcia, B. Ballestreros, J. M. Serra and J. L. Santiso, *Solid State Ionics*, 2012, **216**, 25.
14 M. Huse, A. W. B. Skilbred, M. Karlsson, S. G. Eriksson, T. Norby, R. Haugsrud and C. S. Knee, *J. Solid State Chem.*, 2012, **187**, 27.
15 A. Mielewczyk, K. Gdula-Kasics, B. Kusz and M. Gazda, *Ceram. Int.*, 2013, **39**, 4239.
16 H. Zhang and J. F. Banfield, *J. Phys. Chem. B*, 2000, **104**, 3481.

17 A. A. Gribb and J. F. Banfield, *Am. Mineral.*, 1997, **82**, 717.

18 S. Shukla and S. Seal, *Int. Mater. Rev.*, 2005, **50**, 1.

19 F. Maglia, I. Tredici and U. Anselmi-Tamburini, *J. Eur. Ceram. Soc.*, 2013, **33**, 1045.

20 N.-L. Wu, T.-F. Wu and I. A. Rusakova, *J. Mater. Res.*, 2001, **69**, 666.

21 M. W. Pitcher, S. V. Ushanov, A. Navrotsky, B. F. Woodfield, G. Li, J. Boerio-Goates and B. M. Tissue, *J. Am. Ceram. Soc.*, 2005, **88**, 160.

22 M. Amsif, D. Marrero-Lopez, J. C. Ruiz-Morales, S. Savvin and P. Nunerz, *J. Eur. Ceram. Soc.*, 2012, **32**, 1235.